

NOISE-AWARE QUANTUM AMPLITUDE ESTIMATION

STEVEN HERBERT^{1,2}, ROLAND GUICHARD¹, DARREN NG¹

¹ *Quantinuum (Cambridge Quantum), Terrington House, 13-15 Hills Rd, Cambridge, CB2 1NL, UK*

² *Department of Computer Science and Technology, University of Cambridge, UK*

ABSTRACT. In this paper we derive from simple and reasonable assumptions a Gaussian noise model for Quantum Amplitude Estimation (QAE). We provide results from QAE run on various IBM superconducting quantum computers and Quantinuum’s H1 trapped-ion quantum computer to show that the proposed model is a good fit for real-world experimental data. We then give a generalised procedure for how to embed this noise model into any quantum phase estimation-free QAE algorithm, such that the amplitude estimation is “noise-aware”.

I. INTRODUCTION

The term *noisy intermediate-scale quantum [computer]* (NISQ), coined by John Preskill [1] has become the industry standard for early quantum computers, and the name immediately tells us two of their most important features: they are noisy, and they are too small (“intermediate-scale”) to run fault-tolerant algorithms. Thus noise, and the consequent possibility of error, is something we have to live with.

Many ingenious suggestions for error *mitigation* (that is, using circuit design and classical pre- and post-processing to reduce the adverse effects of noise, without actually using any qubits for quantum error correction) have been proposed, including *zero-noise extrapolation* [2,3], *randomised compilation* [4], *probabilistic error correction* [5] and many more. It is also likely that some quantum error correction (albeit falling short of the amount required for fault-tolerance) will ultimately be deployed in early algorithms exhibiting genuine useful quantum advantage (e.g. Refs. [6,7]), and so it is perhaps more appropriate to speak of *resource-constrained* quantum hardware, where the aim of algorithm design is to achieve such quantum advantage with minimal resource requirements.

One approach (which in general is complementary to the error mitigation techniques discussed above) is to characterise the noise as a “noise model” and handle the noise at the application level. This is particularly applicable for quantum sampling algorithms (e.g. Refs. [8–11]), where the effect of the noise is that the samples are from a different distribution than in the corresponding noiseless case, but in principle with an accurate noise model the distribution actually being sampled from can still be expressed. Moreover,

sampling provides the basis for many quantum optimisation and estimation algorithms [8,9], and with an accurate noise model there may still be quantum advantage in speed of convergence even in the presence of noise (that is, if the noise is sufficiently mild, with some errors possibly having been mitigated / corrected by some of the techniques mentioned).

In this paper we address what is probably the simplest such instance of this concept, by proposing a suitable model for the noise accumulated when Grover iterations are repeated to perform quantum amplitude amplification. In particular, we address one such algorithm, quantum amplitude estimation (QAE), and focus on propositions for QAE, which do not call quantum phase estimation (QPE) as a subroutine [12–15]. Thus, in these algorithms the quantum circuits consist only of state preparation and then amplitude amplification, there is no other circuitry involved. Moreover, these proposed algorithms all share the property that only a single qubit is measured, which gives us the basis for a simple Gaussian noise model. Additionally, QAE not only provides a suitable subject for a noise model, but is also an important algorithm which underpins quantum Monte Carlo integration (QMCI) [8,16–18], and thus forms the basis for many important anticipated applications in, for example, quantum finance [19–29].

This approach of translating the noise at the physical level to the resultant estimation uncertainty at the application level in QAE has begun to gain traction in recent months, with both Brown *et al* [30] and Tanaka *et al* [31] investigating how generic noise models such as depolarising, amplitude damping and phase damping noise impact the performance of *Amplitude Estimation without Phase Estimation* [12]. The results we present in this paper are complementary to, and in some ways extend, these results. In particular, to our knowledge this is the first time that

Contact: Steven.Herbert@cambridgequantum.com

a noise model specific to QAE has been derived, even though the aforementioned papers note the importance (and difficulty) of doing so (“It is indeed a difficult challenge to model a noise effect” Ref. [31, Section 5]; “... any lack of accuracy in one’s noise characterisation will translate to a lack of accuracy in amplitude estimation. Understanding better this difficulty represents a fruitful line of future research.” Ref. [30, Section IV-A]). Moreover, a noise model is a statistical characterisation of some physical process, and hence stands independently of any particular flavour of QAE, and instead provides a quantification of the measurement uncertainty that can then be used to more accurately infer the amplitude from the measured data. To this end, our main example for how to use the proposed noise model to achieve noise-aware QAE concerns a quantification of the number of additional shots that are needed, given the circuit depth, to achieve the same variance as the noiseless case. This applies across the board to all QPE-free QAE algorithms, which all use repeated shots of the same circuit are used to infer the amplitude, including some recent suggestions for shallow-depth QAE [32, 33].

Looking more broadly at QPE-free QAE, Wang *et al* [34] take a different approach and cast QAE as an instance of generic observable measurement. They take an adaptive, Bayesian approach, showing that by tuning the circuit parameters adaptively as the parameters become known with greater confidence, in turn the future expected information gain can be maximised. In future work it will be interesting to see if, and to what extent, the bespoke noise model we propose here can further enhance the Bayesian approach to quantum sampling – however this is beyond the scope of the present paper. It is also worth noting that efforts are afoot to investigate the performance of QAE on noisy quantum computers, even without application-level handling of the noise [35].

Paper organisation. The remainder of the paper is organised as follows: in Section II we describe in detail how the Gaussian noise model is derived from some reasonable initial assumptions – and also demonstrate that depolarising noise is a special case of the Gaussian noise model; in Section III we present a series of experiments, run on actual quantum hardware, to probe the real-world applicability of our proposed noise-model; then in Section IV we include and discuss the results of these experiments; in Section V we give the theory and general framework for our proposed noise-aware QAE algorithm; in Section VI we give some further numerical results for the noise-aware QAE algorithm; and finally in Section VII we draw conclusions.

II. THEORETICAL DERIVATION OF THE GAUSSIAN NOISE MODEL

To derive the Gaussian noise model, it is first necessary to introduce QAE [36]: QAE uses a generalisation of Grover’s search algorithm [37], amplitude amplification, to estimate the amplitude, $a = \sin^2 \theta$, of a general n -qubit quantum state expressed in the form:

$$|\psi\rangle = \cos \theta |\Psi_0\rangle |0\rangle + \sin \theta |\Psi_1\rangle |1\rangle \quad (1)$$

for some $(n-1)$ -qubit states $|\Psi_0\rangle$ and $|\Psi_1\rangle$. A circuit, A , which prepares $|\psi\rangle$, that is $|\psi\rangle = A|0^n\rangle$, is taken as the input to the QAE algorithm, from which it is possible to build an operator $Q = -AS_0A^{-1}S_\chi$ (where $S_0 = X^{\otimes n}(C_{n-1}Z)X^{\otimes n}$ and $S_\chi = I_{2^{n-1}} \otimes Z$ do not depend on A) which performs Grover iteration:

$$Q^m |\psi\rangle = \cos((2m+1)\theta)|\Psi_0\rangle|0\rangle + \sin((2m+1)\theta)|\Psi_1\rangle|1\rangle \quad (2)$$

Thus, for m applications of Q , the probability of measuring the state $|1\rangle$ on the last qubit is $\sin^2((2m+1)\theta)$, and the essential idea common to all QPE-free QAE algorithms is to run circuits for a variety of different values of m and then to use classical post-processing to estimate θ and hence a . In the presence of noise each Grover iterate will not necessarily enact a rotation of exactly 2θ and thus we can write the actual rotation enacted by the i^{th} Grover iterate as $2\theta + \epsilon_i$ where ϵ_i is some error, which then gives:

$$|\psi\rangle \xrightarrow{Q^m} \cos\left((2m+1)\theta + \sum_{i=1}^m \epsilon_i\right) |\Psi_0\rangle |0\rangle + \sin\left((2m+1)\theta + \sum_{i=1}^m \epsilon_i\right) |\Psi_1\rangle |1\rangle \quad (3)$$

Note that Equation (3) is a general expression for the state after m Grover iterations: that is, there are no hidden assumptions in treating each Grover iteration to be a rotation by the desired (noiseless) angle plus some additional erroneous component – this is a completely general way of representing the final state of a QAE circuit run on a noisy machine. It is also pertinent that, by treating the Grover iteration as a “black box” in this way, Equation (3) is agnostic to the specific realisation of the algorithm as a quantum circuit – covering even cases where quantum error correction is deployed, for example. In order to turn this into a useful noise model it is necessary to introduce an assumption, namely that the various ϵ_i are independent and identically distributed (i.i.d.) and m is sufficiently large that we can invoke the central limit theorem (CLT) to approximate the sum of the random variables ϵ_i as a single random variable drawn from a Gaussian distribution. In this case that the

state can be expressed:

$$Q^m |\psi\rangle = \cos((2m+1)\theta + \theta_\epsilon) |\Psi_0\rangle |0\rangle + \sin((2m+1)\theta + \theta_\epsilon) |\Psi_1\rangle |1\rangle \quad (4)$$

such that $\theta_\epsilon \sim \mathcal{N}(k_\mu m, k_\sigma m)$, where $\mathcal{N}(\text{mean}, \text{variance})$ is the normal distribution, and k_μ and k_σ are constants. It is worth noting that the assumption that the various ϵ_i are i.i.d. is actually an unnecessarily strong requirement. In fact, all that is required is that a sufficiently large number of independent underlying ‘‘factors’’ contribute to the randomness that a Gaussian random variable well-models the value in question. This assumption is identical to that ubiquitously used in wireless communications literature to model noise as *additive white Gaussian noise* [38].

This noise model applies because we are only interested in the error on a single qubit, and this allows us to use a classically inspired approach and invoke the CLT. The result is a noise model that is somewhat different in appearance to that which may conventionally be derived for modelling noisy quantum channels. In particular, we do not express a mixed state, but rather notice that a mixed state simply captures classical uncertainty about which pure state some quantum system is in. Thus our proposed Gaussian noise model can be thought of as always treating the quantum state as pure, and then quantifying the relevant part of our uncertainty about what that quantum state is separately.

II.1. Depolarising noise is a special case of the Gaussian noise model. Of the existing generic noise models, our proposed Gaussian noise model is most similar to the depolarising noise model. The depolarising noise model supposes that each layer of quantum gates has some probability of completely depolarising the quantum state, whereas the Gaussian noise model supposes that the state gradually depolarises in a continuous manner. However, it turns out that when $k_\mu = 0$ the depolarising noise model and Gaussian noise model are identical, as we now show.

To begin, consider the probability of the measurement outcome being zero in depolarising noise:

$$p(0) = p_{coh}^d \cos^2((2m+1)\theta) + (1 - p_{coh}^d) \frac{1}{2} \quad (5)$$

where p_{coh} is some (fixed) finite probability of the state remaining coherent (not depolarising), and d is the circuit depth. For comparison with the Gaussian noise model it is easiest to express the probability of measuring 1 subtracted from the probability of measuring 0. Using the fact that the circuit depth is

approximately proportional to m we get:

$$\begin{aligned} p(0) - p(1) &= \left(\tilde{p}_{coh}^m \cos^2((2m+1)\theta) + (1 - \tilde{p}_{coh}^m) \frac{1}{2} \right) \\ &\quad - \left(\tilde{p}_{coh}^m \sin^2((2m+1)\theta) + (1 - \tilde{p}_{coh}^m) \frac{1}{2} \right) \\ &= \tilde{p}_{coh}^m (\cos^2((2m+1)\theta) - \sin^2((2m+1)\theta)) \end{aligned} \quad (6)$$

where \tilde{p}_{coh} is an adjusted version of p_{coh} such that the scaling is in terms of number of Grover iterates. We now show that the same asymptotic behaviour occurs in the proposed Gaussian noise model. To do so, first we consider the probability of the measurement outcome being 0 when the noise is Gaussian, which can be expressed:

$$\begin{aligned} p(0) &= \int_{-\infty}^{\infty} p(0|\theta_\epsilon) p(\theta_\epsilon) d\theta_\epsilon \\ &= \int_{-\infty}^{\infty} \cos^2((2m+1)\theta + \theta_\epsilon) \frac{e^{-\frac{(\theta_\epsilon - k_\mu m)^2}{2k_\sigma m}}}{\sqrt{2\pi k_\sigma m}} d\theta_\epsilon \end{aligned} \quad (7)$$

We can similarly express the probability of outcome 1:

$$p(1) = \int_{-\infty}^{\infty} \sin^2((2m+1)\theta + \theta_\epsilon) \frac{e^{-\frac{(\theta_\epsilon - k_\mu m)^2}{2k_\sigma m}}}{\sqrt{2\pi k_\sigma m}} d\theta_\epsilon \quad (8)$$

Next we subtract (8) from (7):

$$\begin{aligned} p(0) - p(1) &= \int_{-\infty}^{\infty} \cos^2((2m+1)\theta + \theta_\epsilon) \frac{e^{-\frac{(\theta_\epsilon - k_\mu m)^2}{2k_\sigma m}}}{\sqrt{2\pi k_\sigma m}} \\ &\quad - \sin^2((2m+1)\theta + \theta_\epsilon) \frac{e^{-\frac{(\theta_\epsilon - k_\mu m)^2}{2k_\sigma m}}}{\sqrt{2\pi k_\sigma m}} d\theta_\epsilon \\ &= \frac{1}{\sqrt{2\pi k_\sigma m}} \\ &\quad \int_{-\infty}^{\infty} \cos(2((2m+1)\theta + \theta_\epsilon)) e^{-\frac{(\theta_\epsilon - k_\mu m)^2}{2k_\sigma m}} d\theta_\epsilon \\ &= \frac{1}{\sqrt{2\pi k_\sigma m}} \mathcal{R} \left(e^{2i(2m+1)\theta} \int_{-\infty}^{\infty} e^{2i\theta_\epsilon} e^{-\frac{(\theta_\epsilon - k_\mu m)^2}{2k_\sigma m}} d\theta_\epsilon \right) \\ &= \frac{1}{\sqrt{2\pi k_\sigma m}} \mathcal{R} \left(e^{2i(2m+1)\theta + 2ik_\mu m} \int_{-\infty}^{\infty} e^{2i\tilde{\theta}_\epsilon - \frac{\tilde{\theta}_\epsilon^2}{2k_\sigma m}} d\tilde{\theta}_\epsilon \right) \\ &= \frac{1}{\sqrt{2\pi k_\sigma m}} \mathcal{R} \left(e^{2i(2m+1)\theta + 2ik_\mu m} \sqrt{2\pi k_\sigma m} e^{-2k_\sigma m} \right) \\ &= e^{-2k_\sigma m} \cos(2((2m+1)\theta + k_\mu m)) \\ &= e^{-2k_\sigma m} \left(\cos^2((2m+1)\theta + k_\mu m) \right. \\ &\quad \left. - \sin^2((2m+1)\theta + k_\mu m) \right) \end{aligned} \quad (9)$$

where \mathcal{R} denotes the real part, and the substitution $\tilde{\theta}_\epsilon = \theta_\epsilon - k_\mu m$ is used to simplify the integral.

We can see that when $k_\mu = 0$ (which is effectively implicit in the depolarising noise model) the depolarising and Gaussian noise models have identical measurement statistics, that is when the parameters are matched accordingly ($\tilde{p}_{coh} \equiv e^{-2k_\sigma}$) Equations (6) and (9) are equivalent. (Note that, as there are only two measurement outcomes, namely 0 and 1, and probabilities sum to one, the measurement statistics are completely determined by the value of $p(0)-p(1)$).

This correspondence between the depolarising and Gaussian noise models is important for a number of reasons:

- The fact that the Gaussian noise model we propose here corresponds to a widely-used and accepted noise model (i.e. depolarising noise) adds credence to its validity.
- Conversely, the fact that the Gaussian noise model has been derived from simple and justified physical assumptions gives a phenomenological (rather than ad-hoc) basis to use the depolarising noise model in appropriate circumstances.
- In our proposed Noise-Aware QAE algorithms (Algorithm 1) we use both the Gaussian and depolarising features of the noise channel to improve the performance of QAE.

II.2. Justification for characterising the noise as a function of the number of Grover iterations.

Whilst the Gaussian noise model derives naturally from some basic and reasonable starting assumptions, it is perhaps wise to pause and ask whether the whole enterprise is fatally flawed, owing to the rigid requirement that the Gaussian iterate circuit remains in place. That is, because the Gaussian noise model explicitly requires a succession of Grover iterates which ostensibly precludes other forms of noise mitigation (for instance combining circuit optimisation and other traditional noise-mitigation schemes). However, a more detailed look at the structure of QAE circuits reveals that such an approach would still leave a repeated sequence of identical (or near-identical) circuit blocks. This is because, once the number of qubits has exceeded that for which the entire unitary could be re-synthesised from scratch¹ all that can be done is a peep-hole type optimisation. In this case, the multi-controlled CZ gate that is central to the Grover iterate circuit (see the text above (2)) acts as a barrier to *too* much

¹As will clearly be the case for problem sizes exhibiting useful quantum advantage – but will actually be the case for rather smaller problem sizes than that, for instance tket [39] only does so for circuits with three qubits or fewer. That said, the examples in the numerical results in this paper are of such a small size, and hence this feature was turned off.

commutation of other gates past these regularly recurring multi-controlled CZ gates, and hence even a re-written circuit would have a similar overall structure.

III. NOISE MODEL EXPERIMENTAL SET-UP

In order to gather experimental results to assess the real-world applicability of the proposed Gaussian noise model, it is necessary to select some state preparation circuits, A , and run QAE on real quantum hardware. For this, we are guided by the following two principles: firstly, we minimise the number of qubits used in A in order that we can run deeper circuits (more applications of Q) which thus allows us to better observe how well the Gaussian noise model fits the experimental data; and secondly we choose circuits which have the property that noiselessly θ is such that on periodic numbers of Grover iterations the measurement outcome is either $|0\rangle$ or $|1\rangle$ with certainty, which allows us to display plots to illustrate how well the noise model fits the experimental data. Two circuits which achieve these aims are A_1 and A_2 , shown in Fig. 1, which prepare the states:

$$A_1 |00\rangle = \cos(\pi/6) |\Psi_0\rangle |0\rangle + \sin(\pi/6) |\Psi_1\rangle |1\rangle \quad (10)$$

$$A_2 |00\rangle = \cos(\pi/3) |\Psi_0\rangle |0\rangle + \sin(\pi/3) |\Psi_1\rangle |1\rangle \quad (11)$$

So we can see that

$$Q_1^m A_1 |00\rangle = \cos((2m+1)\pi/6) |\Psi_0\rangle |0\rangle + \sin((2m+1)\pi/6) |\Psi_1\rangle |1\rangle \quad (12)$$

$$Q_2^m A_2 |00\rangle = \cos((2m+1)\pi/3) |\Psi_0\rangle |0\rangle + \sin((2m+1)\pi/3) |\Psi_1\rangle |1\rangle \quad (13)$$

where Q_1 and Q_2 are the Grover iterate circuits for A_1 and A_2 respectively. We can see that $Q_1^m A_1 |00\rangle$ (resp. $Q_2^m A_2 |00\rangle$) has the property that the measurement of the last qubit is 1 (resp. 0) with certainty when $(m-1) \bmod 3 = 0$ (that is for $m = 1, 4, 7, \dots$). Fig. 2 illustrates this for the case of A_1 . Even though in principle QAE could be applied to a single-qubit circuit, A , the lack of entanglement therein would make it an unsuitable experiment, and thus by selecting 2 qubit circuits, we have used the minimum number of qubits that we can reasonably expect to lead to meaningful results.

Whilst A_1 and A_2 achieve our aim of running simple circuits that lead to results that can readily be plotted, it is also beneficial to include a range of different circuits. To this end we also run QAE for A_1 and A_2 simultaneously (to introduce the possibility of cross-talk) and additionally for A_3 , A_4 and A_5 , also

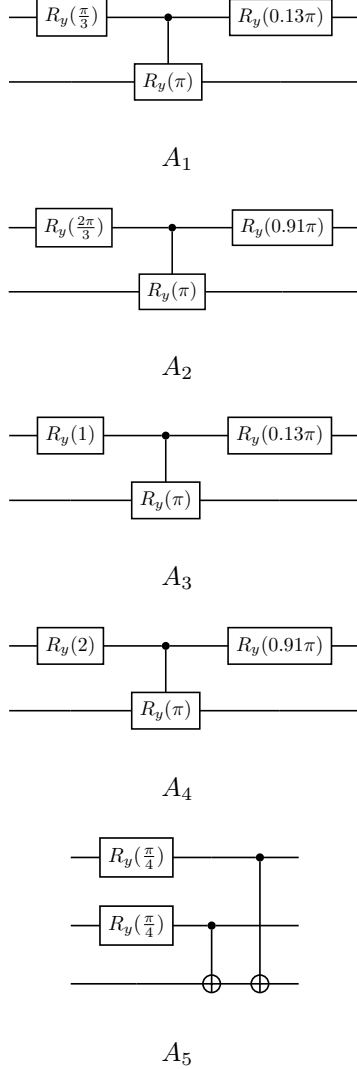


Fig. 1. State preparation circuits.

shown in Fig. 1, which prepare the states:

$$A_3 |00\rangle = \cos(1/2) |\Psi_0\rangle |0\rangle + \sin(1/2) |\Psi_1\rangle |1\rangle \quad (14)$$

$$A_4 |00\rangle = \cos(1) |\Psi_0\rangle |0\rangle + \sin(1) |\Psi_1\rangle |1\rangle \quad (15)$$

A_3 and A_4 are such that the final qubit does not align with the $|0\rangle$ or $|1\rangle$ axes after any number of applications of Q .

A three-qubit circuit, A_5 is also defined (for later use), and prepares the state

$$A_5 |000\rangle = \cos(\pi/6) |\Psi_0\rangle |0\rangle + \sin(\pi/6) |\Psi_1\rangle |1\rangle \quad (16)$$

For the first round of experiments, we ran the QAE circuits for m applications of Q where $m = 0 \dots 67$. This range was set on the basis of preliminary studies to discover the reasonable maximum

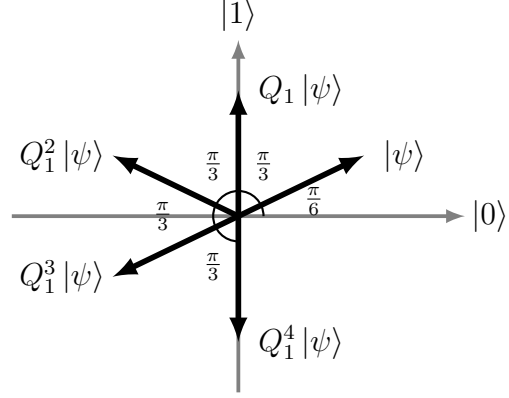


Fig. 2. Illustration of the action of Q_1^m on $|\psi\rangle = A_1 |00\rangle$. Here we show for $m = 0 \dots 4$, but we can easily see that the pattern will repeat after $m = 6$ (i.e. so that we can take m modulo 6 to find the rotation angle).

circuit depths (i.e. before noise becomes overwhelming). For the experiments we used four of IBM’s five-qubit machines (Athens, Bogota, Rome and Santiago – all of the five-qubit machines online at the time of the experiments), each of which uses superconducting qubits connected in a line [40]. Cambridge Quantum Computing’s tket compiler [39] was used to run the circuits – the compiler was set to map the circuit to the physical qubit connectivity and native gate-set but not to perform any “optimisation”, that is circuit re-writing to achieve a functionally equivalent but shallow-depth circuit (compiled circuits shown in Appendix A). In this way, we guaranteed that the circuit executed consisted of the appropriate number of repeated Grover iterations, as is necessary to probe the validity of the proposed noise model.

We used minimum mean-squared error (MMSE) parameter fitting [41, pp 344 – 350] to find the noise-model parameters that best fit the experimental data. That is, each noise model can be expressed as a parameterised family of functions (i.e., measurement outcome probability as a function of number of Grover iterates) and hence the specific instance of the family of functions that minimises the mean squared discrepancy between the experimental values and the values predicted by the noise-model was selected as the ‘best fit’. For each experiment we did this for two noise models: the Gaussian noise model proposed herein; and the depolarising noise model (which is equivalent to the Gaussian noise model with k_μ set to zero, as shown in Section II.1). We ran each circuit for the maximum allowed number of shots, which is 8192. By doing so we were able to simplify the analysis by treating the average of the 8192 shots as exactly

equal to the square of the modulus of the amplitude of the $|1\rangle$ component of the last qubit (that is, when expressed in the form of (2)).

To see why this holds let \hat{p}_1 be the estimate of p_1 we obtain by averaging 8192 shots, then we have that:

$$\hat{p}_1 \sim \mathcal{N}(p_1, p_1(1 - p_1)/8192) \quad (17)$$

using the Gaussian approximation of the binomial (which is clearly valid for the summation of 8192 i.i.d Bernoulli random variables). The standard deviation (square-root of variance) is maximised when $p_1 = 0.5$ which we use to find that the standard-deviation is at most 0.00552, which is extremely small, and means that it is reasonable to use the average of the 8192 shots as exactly p_1 in the following analysis.

For the second round of experiments we used Quantinuum’s H1 trapped-ion quantum computer [42]. Owing to the slower gate times, and more restricted device availability, we were only able to run a smaller measurement campaign than that using the IBM devices. However, because of the superior quantum volume of the Quantinuum machine compared to the IBM devices [43], we were able to confidently run a three qubit circuit, A_5 , also shown in Fig. 1, which prepares the state given in (16).

A_5 has the same “periodic” property as A_1 that noiselessly $Q^m A_5 |000\rangle$ yields measurement outcome 1 with certainty on the third qubit when $(m - 1) \bmod 3 = 0$. Experiments were run for $m = 0, 1, \dots, 12$, and for each circuit, 1024 shots were performed. On a different day, further experiments were run on the Quantinuum machine for $m = 0, 1, \dots, 13$, and for each circuit, 1500 shots were performed. Whilst these numbers of shots are approximately an order of magnitude smaller than in the IBM experiments, it remains acceptable for the argument about neglecting the binomial uncertainty to still hold. The two different rounds of experiments on the Quantinuum machine are denoted “(run 1)” and “(run 2)” respectively in the following.

The experiments using IBM hardware were run in December 2020 and January 2021; the experiments using Quantinuum H1 hardware were run in June and July 2021.

IV. NOISE MODEL RESULTS AND DISCUSSION

From the MMSE-fitted parameters we calculate R^2 values to evaluate the goodness-of-fit of the two noise models under consideration. These R^2 values are given in Table 1 – note that R^2 is at most equal to 1 and $R^2 = 1$ means that all of the experimentally observed variance is explained by the proposed model. Additionally Fig. 3 shows plots for A_1 run on the various IBM machines, with circuit

Circuit	Machine	Gaussian	Depolarising
A_1	Athens	0.9546	0.8052
	Bogota	0.9400	0.5822
	Rome	0.9667	0.8678
	Santiago	0.8936	0.8721
A_2	Athens	0.8821	0.7741
	Bogota	0.8633	0.7857
	Rome	0.6658	0.6323
	Santiago	0.8956	0.8952
A'_1	Athens	0.8967	0.8893
	Bogota	0.8138	0.7584
	Rome	0.5066	0.5061
	Santiago	0.7664	0.7115
A'_2	Athens	0.9110	0.8398
	Bogota	0.7283	0.6659
	Rome	0.8089	0.8072
	Santiago	0.7975	0.7884
A_3	Athens	0.9899	0.9831
	Bogota	0.7763	0.6743
	Rome	0.8890	0.6121
	Santiago	0.9260	0.8638
A_4	Athens	0.8876	0.8527
	Bogota	0.8755	0.8038
	Rome	0.8040	0.7290
	Santiago	0.8619	0.8179
A_5	H1 (1)	0.9846	0.9841
	H1 (2)	0.9671	0.9612

Table 1. R^2 values for the various state preparation circuits running on each of the 5-qubit IBM superconducting quantum computers and Quantinuum’s H1 trapped-ion quantum computer (runs 1 and 2 as marked). A'_1 and A'_2 denote the results from A_1 and A_2 respectively when A_1 and A_2 were run simultaneously.

depths $m = 1, 4, 7, \dots$ (i.e. number of Grover iterates such that the noiseless measurement outcome is always equal to 1); and Fig. 4 shows plots for A_1 run on the various machines, with circuit depths $m = 0, 2, 3, 5, 6, 8, 9, \dots$ (i.e. number of Grover iterates such that the noiseless measurement outcome is equal to zero with probability 0.75).

From these results it is immediately apparent that, as emphasised by the bold font in Table 1, the proposed Gaussian noise model (with variable mean) is invariably a better fit than the depolarising noise model (Gaussian noise model with mean fixed at zero). This is because the Gaussian noise model with parameterised mean can capture a constant “bias” or “drift” where each Grover iterate performs a rotation which is offset from the theoretical rotation angle by

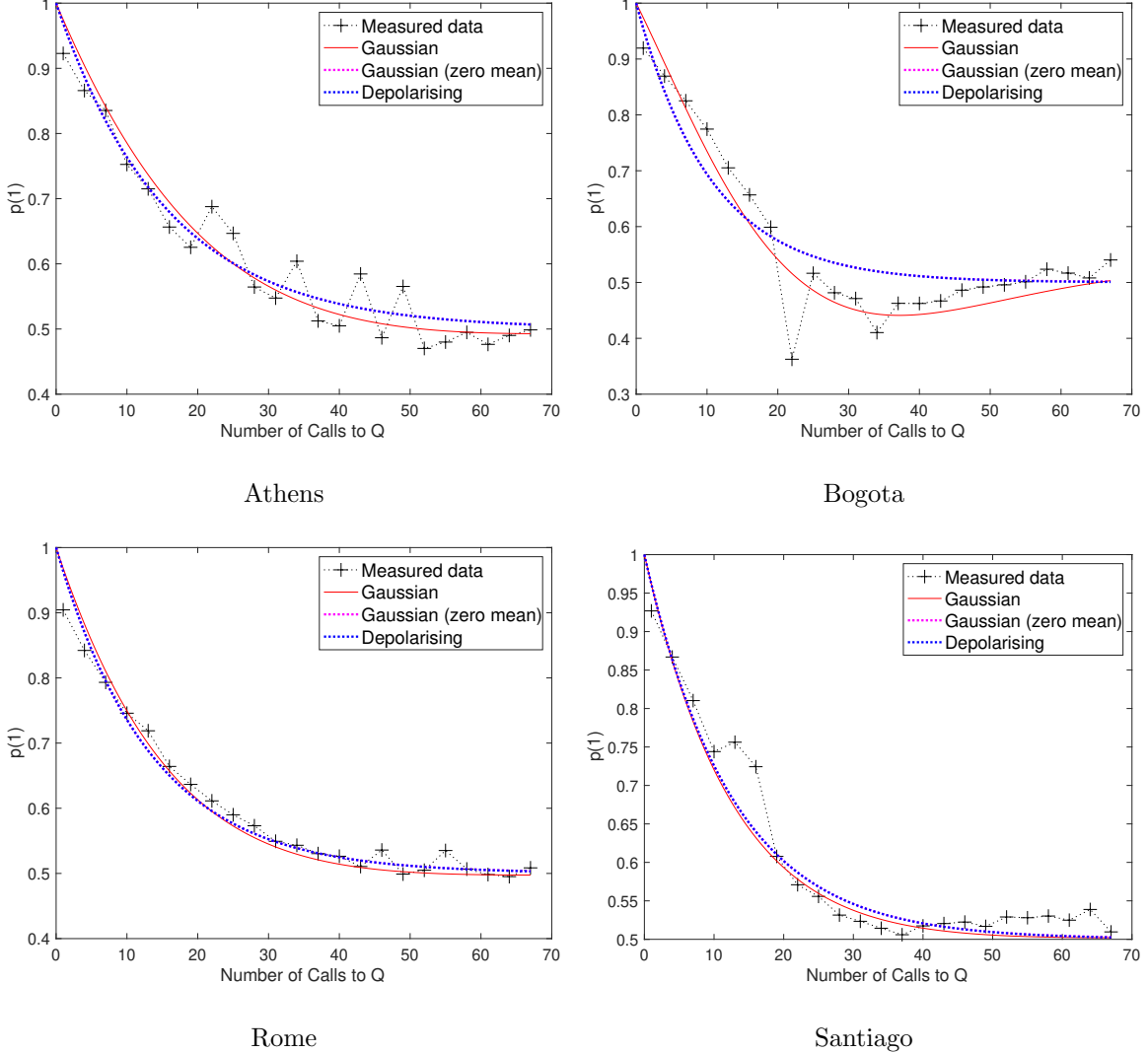


Fig. 3. A_1 run on each of the four 5-qubit IBM machines: results plotted for 1, 4, 7, ... Grover iterations (that is, iterations where in the absence of noise the measurement outcome would be 1 with certainty).

some constant amount (plus some zero-mean random noise). The results for rotation angles $\pi/6$ or $\pi/3$ (as in A_1 , A_2 and A_5) clearly illustrate this, as the constant offset is manifested as the probability of measuring zero (or one) being alternately higher and lower (as the number of Grover iterations is incremented) than the simple depolarising case, as shown in Fig. 4 (specifically, Fig. 4 illustrates that noiselessly for all m such that $(m - 1) \bmod 3 \neq 0$ the probability of measurement outcome being $|0\rangle$ is 0.75). To see an example of this effect, consider the case of a small positive offset to the rotations in Fig. 2. In the case of Q^2 this offset would move the superposition closer to the direction $-|0\rangle$, and so there would a corresponding increase in the probability of measuring 0;

conversely, in the case of Q^3 the offset would move the superposition closer to the direction $-|1\rangle$, and so there would be a corresponding increase in the probability of measuring 1. Thus we can see the grounds for the oscillation observed in Fig. 4. Most strikingly, for A_1 run on Bogota the Gaussian noise model (with variable mean) has $R^2 = 0.9400$ – thus explaining almost all of the experimental data – whereas the depolarising noise model has a much lower R^2 of 0.5822. It should also be noted that, whilst less amenable to visualisation, the same principle explains the better fit of the Gaussian noise model with parameterised mean for A_3 and A_4 .

We can also see that in general the Gaussian noise model is a good fit for the the larger 3-qubit circuit,

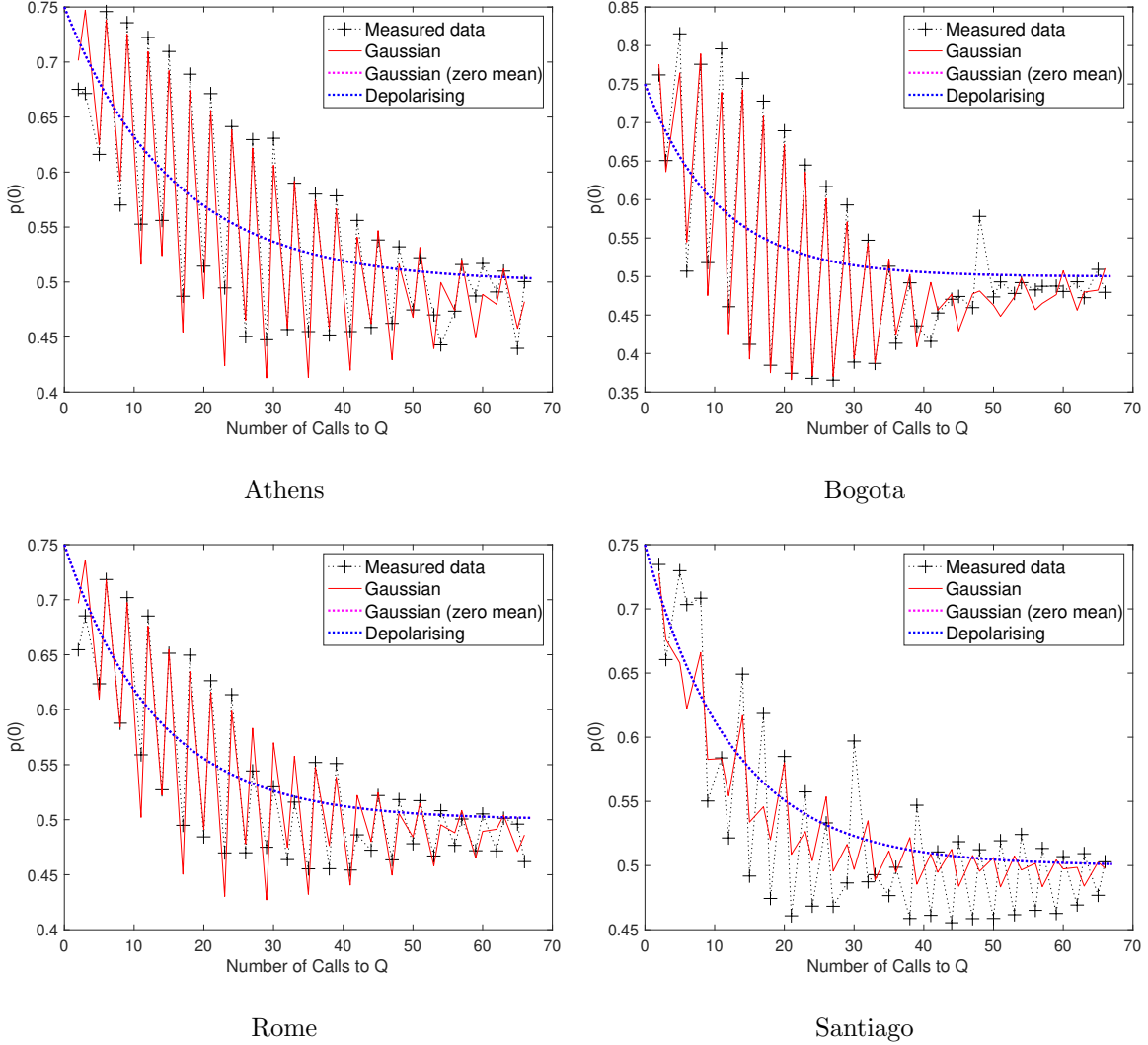


Fig. 4. A_1 run on each of the four 5-qubit IBM machines: results plotted for 2, 3, 5, 6, ... Grover iterations (that is, iterations where in the absence of noise the measurement outcome would be 0 exactly 0.75 of the time).

A_5 . Here we have results from Quantinuum’s machine – a fundamentally different physical manifestation of quantum computation – whose errors also seem to be reasonably well-captured by the Gaussian noise model, as illustrated also in Fig. 5. Note that the R^2 values are consistently higher than those for the superconducting quantum computers owing to the fact that the circuits run were much less deep (there was “less variation to be explained”).

To further analyse the results, there is merit in discussing the goodness-of-fit of the proposed Gaussian noise model from both a phenomenological and operational point of view. Regarding the former, the predictions of the noise model clearly do not explain *all* of the variation observed in the experimental

data (that would correspond to $R^2 = 1$ for all experiments), and thus we can conclude that there are underlying physical causes of the variation not captured by the model. It is worth remarking that the fact that the proposed Gaussian noise model does not capture *everything* is to be expected, as the experiments were explicitly designed to capture raw data from the quantum hardware, and so do not even accommodate the correction of “state preparation and measurement” (SPAM) errors, for instance.

Indeed, Fig. 6 shows the two occasions when the R^2 value is particularly low, and SPAM error is a plausible explanation for each. In the case of A_2 on Rome, we can see that the experimental data does not converge to $p(0) = 0.5$ as the number of Grover

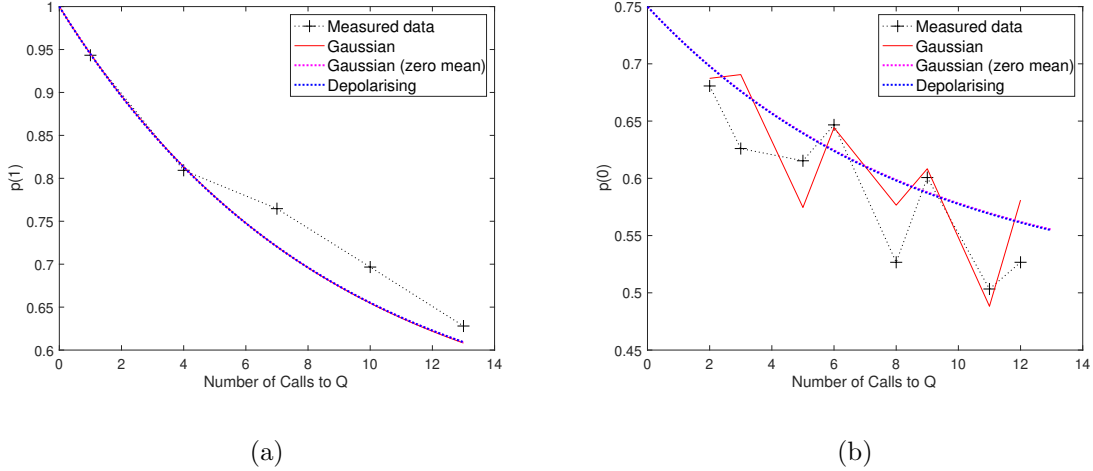


Fig. 5. A_5 run on Quantinuum H1 (run 2): (a) results plotted for 1, 4, 7, ... Grover iterations (that is, iterations where in the absence of noise the measurement outcome would be 1 with certainty); (b) results plotted for 2, 3, 5, 6, ... Grover iterations (that is, iterations where in the absence of noise the measurement outcome would be 0 exactly 0.75 of the time).

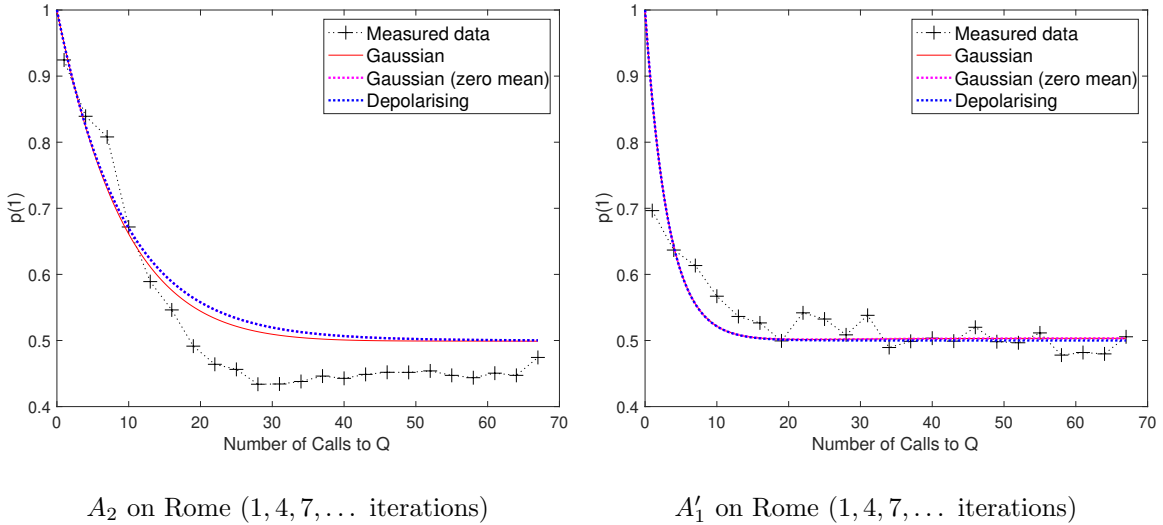


Fig. 6. Plots for occasions when R^2 indicates that the Gaussian noise model is a poor fit.

iterations grows large – a property of all three of the noise models being considered (as the state after a large number of Grover iterations will be close to maximally mixed). One possible explanation for this (there could be others) is that there is a readout error, where (in this case) a bit-flip from 1 to 0 is more likely than the converse – which can be thought of as a type of SPAM error. In the case of A'_1 on Rome, even for a shallow circuit that does little more than simply prepare and measure a state, we have that $p(1) = 0.7$ rather than ≈ 1 , so clearly – indeed, almost by definition – there is a SPAM error.

We now turn to the operational benefits of the Gaussian noise model, which are twofold. Firstly, the fact that the proposed noise model *does* capture the bias is likely to be important for calibration – and furthermore calibration is very important in QAE, as a constant bias cannot be observed (that is, as we are trying to estimate the angle θ from which the amplitude can be found, if θ is perturbed by some constant offset, θ_c , then QAE will simply return the value of $\sin^2(\theta + \theta_c)$ – and no increase to the number of shots will change this). Secondly, we note that the Gaussian noise model is parameterised in a way that can readily be used in the application – as expounded on

in detail in the next two sections. This corresponds to our original motivation to model the noise such that it can be handled at the application level.

Whilst the key quantities for assessing how well the theoretical noise models fit the experimental data are indeed the R^2 values, the parameter values themselves may also be of general interest, and these are included in Table 2 in Appendix B.

V. NOISE-AWARE QAE: THEORY

We now turn our attention to how this noise model can be used to improve amplitude estimates. In particular, we show how the Gaussian noise model can be used to derive a rule for the necessary factor increase in the number of shots required to counteract the noise at a certain circuit depth. To do this, we assume that, even at the maximum circuit depth, the error θ_ϵ is a “small angle”; and also that $k_\mu = 0$ (something that could in principle be achieved by calibration of the machine) and k_σ is exactly known from device characterisation – although in the proposed algorithm we relax this assumption and merely require there to be an initial *prior* probability distribution on k_σ .

Consider that the measurement outcome for a single shot of a circuit with some m Grover iterations is Bernoulli distributed with parameter $\sin^2((2m+1)\theta + \theta_\epsilon)$, using the aforementioned small angle assumption we get:

$$\begin{aligned} \sin^2((2m+1)\theta + \theta_\epsilon) &= \frac{1 - \cos(2((2m+1)\theta + \theta_\epsilon))}{2} \\ &= \frac{1}{2} \left(1 - \cos(2(2m+1)\theta) \cos(2\theta_\epsilon) \right. \\ &\quad \left. + \sin(2(2m+1)\theta) \sin(2\theta_\epsilon) \right) \\ &\approx \frac{1}{2} \left(1 - \cos(2(2m+1)\theta) \right. \\ &\quad \left. + 2\theta_\epsilon \sin(2(2m+1)\theta) \right) \\ &= \sin^2((2m+1)\theta) \\ &\quad + \theta_\epsilon \sin(2(2m+1)\theta) \end{aligned} \quad (18)$$

Next we note that, by the Gaussian noise model, θ_ϵ is normally distributed, with zero mean (by the previous assumption of calibration), and variance $k_\sigma m$, and because $\sin(2(2m+1)\theta)$ is a constant whose magnitude is at most equal to one, it therefore follows that $\theta_\epsilon \sin(2(2m+1)\theta)$ is also normally distributed:

$$\theta_\epsilon \sin(2(2m+1)\theta) \sim \mathcal{N}(0, \sigma^2) \quad (19)$$

where $\sigma^2 \leq k_\sigma m$.

Next we let $\alpha_m = \sin^2((2m+1)\theta)$ be the amplitude of the qubit after m Grover iterates, and let

N_m be the number of shots of this circuit. There are various ways in which the measurement outcomes for all of the different values of m can be combined to infer θ (and hence a), and so to keep things general here we simply assume that the objective is to use the N_m shots to provide a point estimate of α_m , which we denote $\hat{\alpha}_m$. It is worth noting that this assumption, whilst simplistic, is likely to be sufficient to give a good guideline for how to increase the number of shots with m , certainly in the context of other assumptions that have already been made. We use the maximum likelihood estimate of α_m , which is simply the mean of the N_m samples, and using a Gaussian approximation of the binomial distribution, we get that our estimate of the amplitude is normally distributed according to:

$$\hat{\alpha}_m \sim \mathcal{N} \left(\alpha_m + \frac{1}{N_m} \sum_{i=1}^{N_m} \theta_\epsilon^{(i)} \sin(2(2m+1)\theta), \tilde{\sigma}^2 \right) \quad (20)$$

where $\tilde{\sigma}^2 \leq 1/(4N_m)$, using the fact that a Bernoulli random variable has variance at most one quarter. However, when the mean of a Gaussian is itself normally distributed, it is easy to express the resultant distribution,

$$\hat{\alpha}_m \sim \mathcal{N} \left(\alpha_m, \frac{1}{N_m} \sigma^2 + \tilde{\sigma}^2 \right) \quad (21)$$

If we let N_{shot} be the number of shots that would have been selected in the noiseless case (where $k_\sigma = 0$), then we can express the factor increase required to obtain the same estimation worst-case variance for the estimate of α_m :

$$\begin{aligned} \frac{1}{4N_{shot}} &= \frac{4k_\sigma m + 1}{4N_m} \\ \implies N_m &= (4k_\sigma m + 1)N_{shot} \end{aligned} \quad (22)$$

It is worth further remarking the sum in (20) can be thought of as further loop of summation of the errors, ϵ associated with *each* Grover iterate, (as in (3)) and hence “compounds” the use of the CLT, making the assumption of Gaussianity more plausible when the underlying noise model is used in this way.

There is a second way in which the noise model can enhance QAE, namely by improving the parameter inference. Specifically, assuming there is no bias, (or if there is that it has been corrected by prior calibration) it is possible to use the N_m measurement outcomes to recover a typical instance of N_m measurement outcomes that we may have obtained without noise. In particular, using the equivalence between the Gaussian noise model with mean set to zero and depolarising noise, we have that:

$$p(1) = \tilde{p}_{coh}^m \tilde{p}(1) + \frac{1}{2} (1 - \tilde{p}_{coh}^m) \quad (23)$$

where as before $p(1)$ is the probability of measuring one in the presence of depolarising noise, and $\tilde{p} = \sin((2m + 1)\theta)$ is the corresponding noiseless probability. This can easily be rearranged to give:

$$\tilde{p}(1) = \frac{1}{\tilde{p}_{coh}^m} (p(1) - \frac{1}{2} (1 - \tilde{p}_{coh}^m)) \quad (24)$$

Thus, if we have $N^{(1)}$ “ones” amongst our N_m measurement outcomes, then we can predict that we may have measured approximately

$$\tilde{N}^{(1)} = \frac{1}{\tilde{p}_{coh}^m} \left(N^{(1)} - \frac{N_m}{2} (1 - \tilde{p}_{coh}^m) \right) \quad (25)$$

ones in the noiseless case.

We can use these two features to give a general framework for embedding noise-awareness into QPE-free QAE, as shown in Algorithm 1. If Lines 2, 3 and 5 are omitted and $p(\theta, k_\sigma)$ is reinterpreted as simply the marginal probability $p(\theta)$ then we can see that this is a generic framework covering all QPE-free QAE algorithms. Note that normally, but not exclusively, the initial value of m is zero, also note that all QPE-free QAE algorithms implicitly set a uniform prior for θ between 0 and $\pi/2$. It is also the case that this algorithm covered the scenario when k_σ is known exactly *a priori*, as this certainty can easily be encoded in the prior, and the remainder of the algorithm will play out using the corresponding value of k_σ as a constant input. It is also worth highlighting that the framework set out in Algorithm 1 captures both adaptive and non-adaptive QAE: in Line 9 the update to m and N_{shots} can either be done by following a pre-set list, or according to some design based on the current uncertainty of θ . Finally, it is interesting to note that noise-aware QAE uses both the Gaussian and depolarising features of the noise model: the adjustment in N_{shots} is only possible because the noise and the spread around the mean owing to a finite number of shots are both approximately Gaussian in nature; whereas the adjustment of $N^{(1)}$ amounts to an easy deconvolution of the noise, owing to its depolarising nature.

VI. NOISE-AWARE QAE: RESULTS

To assess the performance of noise-aware QAE, we re-use the results of the existing experiment running circuit A_5 on Quantinuum’s H1 trapped-ion quantum computer, and use the measurement outcome results for each of $\{0, 1, 2, 3, 4, 5, 6, 7, 8, 9, 10, 11, 12\}$ uses of A . This is a “linearly increasing sequence” in the terminology of Ref. [12] – although it is important to note that we are using this to have the maximum number of data points (i.e. an m for every integer) rather than because it is the best-performing way to

Algorithm 1 Noise-aware QAE

Require: Quantum circuit A ; prior $p(\theta, k_\sigma)$

- 1: Set m, N_{shots}
 - 2: From $p(\theta, k_\sigma)$ obtain point-estimate, \hat{k}_σ , of k_σ
 - 3: Adjust N_{shots} according to (22) using \hat{k}_σ
 - 4: Prepare and measure N_{shots} of $Q^m A |0\rangle$
 - 5: Adjust $N^{(1)}$ according to (25), using $\tilde{p}_{coh} \equiv e^{-2\hat{k}_\sigma}$
 - 6: Update $p(\theta, k_\sigma)$ using measurement outcomes
 - 7: **if Stopping Criterion** is met **then**
 - 8: Return $\hat{\theta}$
 - 9: **else** Update m, N_{shots} ; Goto Line 2
 - 10: **end if**
-

run QAE. As Suzuki *et al* only specify that a constant number of shots should be used for each element of the sequence, not a specific value, we choose 20 – which we will see is sufficient in the noiseless case. Even using only 20 shots, the data we collected only suffices to give us 14 independent runs of noise-aware QAE for run 1 and 20 independent runs of noise-aware QAE for run 2 (that is, when the increase in N_m to counteract the noise is included), nevertheless this is enough to give us some indication of the benefits of noise-aware QAE. One may suggest that using data from the IBM experiments would be better, as more shots of each circuit were executed, however Quantinuum has two distinct advantages: firstly, the much higher quantum volume gives us more interesting results (even *noise-aware* QAE can only do so much to lift results that dive into the noise floor almost immediately); and secondly, Quantinuum’s machine was observed to have an almost zero bias (that is, $k_\mu \approx 0$), which eliminates the need for “calibration”.

We use the experimental data to compare five settings, as shown in Fig 7: QAE with $N_m = 20$, and no use of the noise model in the parameter estimation, labelled “Vanilla”; QAE with $N_m = 20$, but where the noise model was used to adjust the received data (i.e. Line 5 of Algorithm 1) but not to adjust the number of shots – this amounts to what could realistically be done using a depolarising noise model alone (that is, without the corresponding Gaussian) and is labelled “ $N^{(1)}$ -adjusted”; noise-aware QAE, but where k_σ was set to exactly equal that found from the entire dataset (and so k_σ was not “learned” throughout the algorithms run, but set to the “true” value $k_\sigma^{(true)}$ – given in Table 1), labelled “Known k_σ ”; full noise-aware QAE, where the prior $p(\theta, k_\sigma)$ was set uniformly over $0, \dots, \pi/2$ for θ and $0.5k_\sigma^{(true)}, \dots, 1.5k_\sigma^{(true)}$, labelled “full noise-aware”;

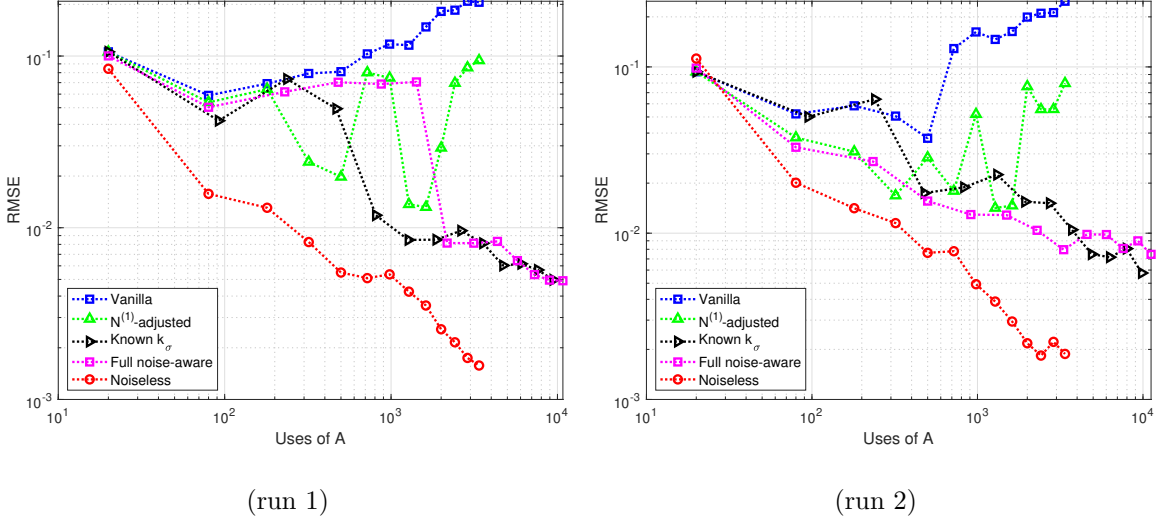


Fig. 7. QAE for various settings for the two experiments (run 1 and run 2) using Quantinuum’s machine: Vanilla QAE with no noise-awareness; $N^{(1)}$ -adjusted using just the depolarising noise model to adjust $N^{(1)}$ according to (25); Known k_σ where k_σ was treated as a constant input; full noise-aware QAE where k_σ was learned on the fly; and noiseless, where simulated results show the theoretical performance on a simulated ideal quantum computer.

and finally, for comparison we simulated a noiseless quantum computer running QAE with $N_m = 20$.

In the case of noise-aware QAE with k_σ set to its “true” value, we found that the number of shots varied as $N_m = 20, 24, 29, 33, 38, 42, 46, 51, 55, 60, 64, 68, 73$ and $N_m = 20, 25, 29, 34, 39, 44, 48, 53, 58, 62, 67, 72, 75$ for $m = 0, 1, \dots, 12$ for run 1 and run 2 respectively (we omitted $m = 13$ for run 2 for consistency, and to be able to average over more runs). In the case where k_σ was learned on the fly, the data points shown are for the average number of shots across all of the runs.

As mentioned above, these results should be taken as indicative only, owing to the small number of QAE runs, but nevertheless we can see the benefits of using the noise model. Without using the noise model at all (even in the parameter estimation) QAE completely fails to converge on the amplitude, whereas even with the noise model only used in the parameter estimation, some initial reduction in RMSE can be seen. However, we can clearly see that the convergence only continues if the noise model is used to adjust N_m such that more shots are executed when the increment noise becomes more severe. Perhaps most encouragingly, even with a relatively high-degree of ignorance about k_σ assumed, the performance is comparable between full noise-aware QAE and that when

k_σ^{true} is used. Using published device information (fidelity, quantum volume etc.) along with coarse information about the circuit, A , we conjecture that it should be possible to set a prior on k_σ which allows noise-aware QAE to work successfully. It also appears to be the case that noise-aware QAE continues to give decent results in practice, even when the small angle assumption no longer holds: for instance, using k_σ from Table 2 we get that the standard deviation in the angle is about 0.8 radians for $m = 12$ (for both run 1 and run 2), which cannot reasonably be called a “small angle”, even though Fig. 7 shows decent convergence at this number of Grover iterations.

The final line, “noiseless” QAE, however, shows there is still some way to go. The challenge now is to use the proposed Gaussian noise model, together with ever-improving quantum hardware, to obtain compelling QAE results for problems of real-world interest. Furthermore, the linearly increasing sequence of Suzuki *et al* is known to not be optimal, and is only really used here for illustrative purposes. An important future line of research and development, therefore, will be to embed the noise model into other proposals for QPE-free QAE to obtain noise-aware versions of the state-of-the-art QPE-free QAE algorithms.

VII. CONCLUSIONS

In this paper we have proposed a simple Gaussian noise model that applies to QPE-free QAE. We have run a number of experiments on various IBM superconducting quantum computers and Quantinuum’s H1 trapped-ion quantum computer to verify the model on real hardware. The proposed Gaussian noise model fits the experimental data well and, notably, captures the bias of the rotation angle, that the generic noise models do not. We have further shown how our proposed noise model can be used to inform the design of, and improve the parameter estimation in, QAE – yielding an algorithm for noise-aware QAE.

An important future direction of research is to combine noise-aware QAE with traditional techniques for error mitigation, and to assess how much further improvement the two complementary approaches give in combination.

ACKNOWLEDGEMENT

The authors thank Cristina Cirstoiu for helpful conversations leading to the development and refinement of the theoretical model, and Ross Duncan for reviewing.

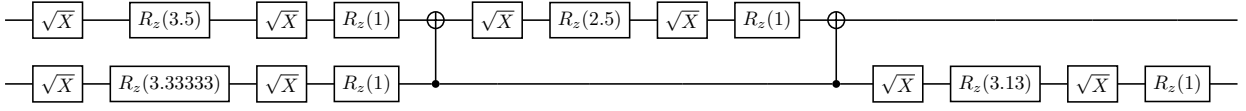
REFERENCES

- [1] J. Preskill, “Quantum computing in the NISQ era and beyond,” *Quantum*, vol. 2, p. 79, Aug 2018. [Online]. Available: <http://dx.doi.org/10.22331/q-2018-08-06-79>
- [2] K. Temme, S. Bravyi, and J. M. Gambetta, “Error mitigation for short-depth quantum circuits,” *Physical Review Letters*, vol. 119, no. 18, Nov 2017. [Online]. Available: <http://dx.doi.org/10.1103/PhysRevLett.119.180509>
- [3] Y. Li and S. C. Benjamin, “Efficient variational quantum simulator incorporating active error minimization,” *Physical Review X*, vol. 7, no. 2, Jun 2017. [Online]. Available: <http://dx.doi.org/10.1103/PhysRevX.7.021050>
- [4] J. J. Wallman and J. Emerson, “Noise tailoring for scalable quantum computation via randomized compiling,” *Physical Review A*, vol. 94, no. 5, Nov 2016. [Online]. Available: <http://dx.doi.org/10.1103/PhysRevA.94.052325>
- [5] S. Endo, S. C. Benjamin, and Y. Li, “Practical quantum error mitigation for near-future applications,” *Physical Review X*, vol. 8, no. 3, Jul 2018. [Online]. Available: <http://dx.doi.org/10.1103/PhysRevX.8.031027>
- [6] A. Holmes, M. R. Joka, G. Pasandi, Y. Ding, M. Pedram, and F. T. Chong, “Nisq+: Boosting quantum computing power by approximating quantum error correction,” in *2020 ACM/IEEE 47th Annual International Symposium on Computer Architecture (ISCA)*, 2020, pp. 556–569.
- [7] R. Majumdar and S. Sur-Kolay, “Special session: Quantum error correction in near term systems,” in *2020 IEEE 38th International Conference on Computer Design (ICCD)*, 2020, pp. 9–12.
- [8] A. Montanaro, “Quantum speedup of monte carlo methods,” *Proceedings of the Royal Society A: Mathematical, Physical and Engineering Sciences*, vol. 471, no. 2181, p. 20150301, 2015. [Online]. Available: <https://royalsocietypublishing.org/doi/abs/10.1098/rspa.2015.0301>
- [9] F. G. S. L. Brandão, A. Kalev, T. Li, C. Y.-Y. Lin, K. M. Svore, and X. Wu, “Quantum sdp solvers: Large speedups, optimality, and applications to quantum learning,” 2019.
- [10] S. Aaronson and A. Arkhipov, “The computational complexity of linear optics,” 2010.
- [11] A. N. Chowdhury and R. D. Somma, “Quantum algorithms for gibbs sampling and hitting-time estimation,” 2016.
- [12] Y. Suzuki, S. Uno, R. Raymond, T. Tanaka, T. Onodera, and N. Yamamoto, “Amplitude estimation without phase estimation,” *Quantum Information Processing*, vol. 19, no. 2, Jan 2020. [Online]. Available: <http://dx.doi.org/10.1007/s11128-019-2565-2>
- [13] D. Grinko, J. Gacon, C. Zoufal, and S. Woerner, “Iterative quantum amplitude estimation,” 2020.
- [14] K. Nakaji, “Faster amplitude estimation,” 2020.
- [15] S. Aaronson and P. Rall, “Quantum approximate counting, simplified,” *Symposium on Simplicity in Algorithms*, p. 24–32, Jan 2020. [Online]. Available: <http://dx.doi.org/10.1137/1.9781611976014.5>
- [16] S. Herbert, “Quantum monte-carlo integration: The full advantage in minimal circuit depth,” 2021.
- [17] —, “Quantum Computing System and Method: Patent application GB2102902.0 and SE2130060-3,” 2021.
- [18] D. An, N. Linden, J.-P. Liu, A. Montanaro, C. Shao, and J. Wang, “Quantum-accelerated multilevel monte carlo methods for stochastic differential equations in mathematical finance,” 2020.
- [19] P. Reberntrost, B. Gupt, and T. R. Bromley, “Quantum computational finance: Monte carlo pricing of financial derivatives,” *Physical Review A*, vol. 98, no. 2, Aug 2018. [Online]. Available: <http://dx.doi.org/10.1103/PhysRevA.98.022321>
- [20] N. Stamatopoulos, D. J. Egger, Y. Sun, C. Zoufal, R. Iten, N. Shen, and S. Woerner, “Option pricing using quantum computers,” 2019.
- [21] S. Woerner and D. J. Egger, “Quantum risk analysis,” *npj Quantum Information*, vol. 5, no. 1, Feb 2019. [Online]. Available: <http://dx.doi.org/10.1038/s41534-019-0130-6>
- [22] A. Bouland, W. van Dam, H. Joorati, I. Kerenidis, and A. Prakash, “Prospects and challenges of quantum finance,” 2020.
- [23] R. Orús, S. Mugel, and E. Lizaso, “Quantum computing for finance: Overview and prospects,” *Reviews in Physics*, vol. 4, p. 100028, 2019. [Online]. Available: <http://www.sciencedirect.com/science/article/pii/S2405428318300571>
- [24] D. J. Egger, R. G. Gutiérrez, J. C. Mestre, and S. Woerner, “Credit risk analysis using quantum computers,” 2019.
- [25] K. Kaneko, K. Miyamoto, N. Takeda, and K. Yoshino, “Quantum pricing with a smile: Implementation of local volatility model on quantum computer,” 2020.
- [26] S. Chakrabarti, R. Krishnakumar, G. Mazzola, N. Stamatopoulos, S. Woerner, and W. J. Zeng, “A threshold for quantum advantage in derivative pricing,” 2020.
- [27] P. Reberntrost and S. Lloyd, “Quantum computational finance: quantum algorithm for portfolio optimization,” 2018.
- [28] D. J. Egger, C. Gambella, J. Marecek, S. McFaddin, M. Mevissen, R. Raymond, A. Simonetto, S. Woerner, and

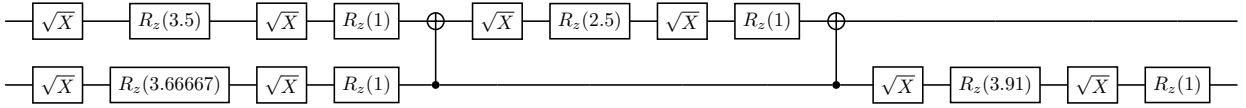
- E. Yndurain, "Quantum computing for finance: State-of-the-art and future prospects," *IEEE Transactions on Quantum Engineering*, vol. 1, pp. 1–24, 2020.
- [29] J. Alcazar, A. Cadarso, A. Katabarwa, M. Mauri, B. Peropadre, G. Wang, and Y. Cao, "Quantum algorithm for credit valuation adjustments," 2021.
- [30] E. G. Brown, O. Goktas, and W. K. Tham, "Quantum amplitude estimation in the presence of noise," 2020.
- [31] T. Tanaka, Y. Suzuki, S. Uno, R. Raymond, T. Onodera, and N. Yamamoto, "Amplitude estimation via maximum likelihood on noisy quantum computer," 2020.
- [32] T. Giurgica-Tiron, I. Kerenidis, F. Labib, A. Prakash, and W. Zeng, "Low depth algorithms for quantum amplitude estimation," 2020.
- [33] I. Kerenidis and A. Prakash, "A method for amplitude estimation with noisy intermediate-scale quantum computers. U.S. Patent Application No. 16/892,229," 2020.
- [34] G. Wang, D. E. Koh, P. D. Johnson, and Y. Cao, "Minimizing estimation runtime on noisy quantum computers," *PRX Quantum*, vol. 2, no. 1, Mar 2021. [Online]. Available: <http://dx.doi.org/10.1103/PRXQuantum.2.010346>
- [35] P. Rao, K. Yu, H. Lim, D. Jin, and D. Choi, "Amplitude estimation algorithms and implementations on noisy intermediate-scale quantum devices," in *OSA Quantum 2.0 Conference*. Optical Society of America, 2020, p. QW6A.16. [Online]. Available: <http://www.osapublishing.org/abstract.cfm?URI=QUANTUM-2020-QW6A.16>
- [36] G. Brassard, P. Hoyer, M. Mosca, and A. Tapp, "Quantum amplitude amplification and estimation," 2000.
- [37] L. K. Grover, "A fast quantum mechanical algorithm for database search," in *Proceedings of the Twenty-Eighth Annual ACM Symposium on Theory of Computing*, ser. STOC '96. New York, NY, USA: Association for Computing Machinery, 1996, p. 212–219. [Online]. Available: <https://doi.org/10.1145/237814.237866>
- [38] V. Garg, *Wireless Communications & Networking*, 1st ed. San Francisco, CA, USA: Morgan Kaufmann Publishers Inc., 2007.
- [39] "TKET." [Online]. Available: <https://github.com/CQCL>
- [40] "IBM quantum computing." [Online]. Available: <https://www.ibm.com/quantum-computing>
- [41] S. M. Kay, *Fundamentals of statistical signal processing: estimation theory*. Prentice-Hall, Inc., 1993.
- [42] "Honeywell quantum solutions." [Online]. Available: <https://www.honeywell.com/us/en/company/quantum>
- [43] "Honeywell quantum volume." [Online]. Available: <https://www.honeywell.com/us/en/news/2021/03/honeywell-sets-new-record-for-quantum-computing-performance>

APPENDIX A. COMPILED CIRCUITS

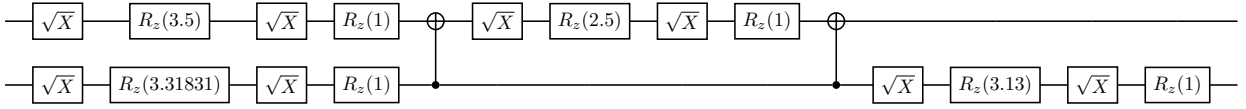
In this appendix we give compiled circuits for A_1, A_2, A_3, A_4, A_5 .



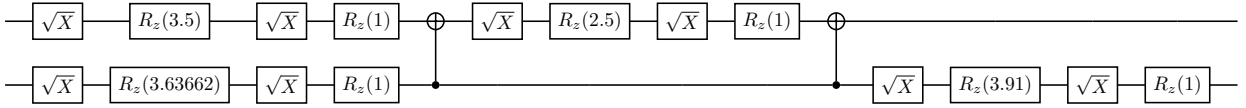
A_1 compiled for IBM



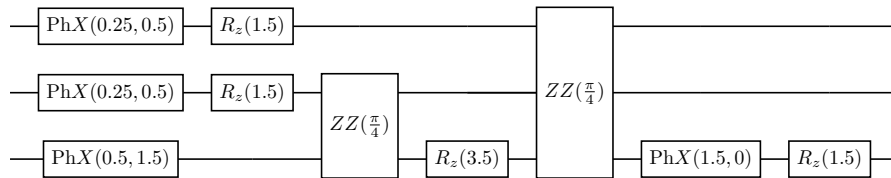
A_2 compiled for IBM



A_3 compiled for IBM



A_4 compiled for IBM



A_5 compiled for Quantinuum H1

APPENDIX B. PARAMETER VALUES FROM THE EXPERIMENTS

In this appendix we give the MMSE parameter values for the two noise models compared in the experiments.

Circuit	Machine	Gaussian		Depolarising	
		k_μ	k_σ	\tilde{p}_{coh}	k_σ
A_1	Athens	0.0152	0.0257	0.9380	0.0320
	Bogota	-0.0335	0.0256	0.9096	0.0474
	Rome	0.0147	0.0326	0.9276	0.0376
	Santiago	-0.0098	0.0400	0.9235	0.0398
A_2	Athens	0.0246	0.0506	0.8792	0.0644
	Bogota	-0.0214	0.0475	0.9038	0.0506
	Rome	-0.0182	0.0532	0.8978	0.0539
	Santiago	-0.0013	0.0423	0.9192	0.0421
A'_1	Athens	0.0053	0.0447	0.9136	0.0452
	Bogota	-0.0129	0.0430	0.9133	0.0454
	Rome	-0.0028	0.1569	0.7299	0.1574
	Santiago	-0.0169	0.0394	0.9182	0.0427
A'_2	Athens	0.0128	0.0331	0.9278	0.0375
	Bogota	-0.0230	0.0644	0.8704	0.0694
	Rome	-0.0061	0.1449	0.7466	0.1461
	Santiago	-0.0081	0.0449	0.9155	0.0441
A_3	Athens	0.0027	0.0244	0.9520	0.0246
	Bogota	-0.0231	0.0478	0.8927	0.0568
	Rome	-0.0359	0.0367	0.8894	0.0586
	Santiago	-0.0189	0.0521	0.8961	0.0549
A_4	Athens	0.0102	0.0374	0.9229	0.0401
	Bogota	0.0132	0.0407	0.9122	0.0459
	Rome	-0.0175	0.0353	0.9233	0.0399
	Santiago	0.0102	0.0288	0.9403	0.0308
A_5	H1 (run 1)	0.0021	0.0553	0.8953	0.0553
	H1 (run 2)	0.0078	0.0581	0.8896	0.0585

Table 2. Parameter values for the various state preparation circuits running on each of the 5-qubit IBM superconducting quantum computers and Quantinuum’s H1 trapped-ion quantum computer. A'_1 and A'_2 denote the results from A_1 and A_2 respectively when A_1 and A_2 were run simultaneously. k_σ under the depolarising noise model was calculated from \tilde{p}_{coh} using the established conversion $k_\sigma = -\log_e(\tilde{p}_{coh})/2$.

As a side-point, we can see from Table 2 that circuits A_1 and A_2 run together (i.e., the rows denoted A_1' and A_2' respectively) have marginally higher depolarising probabilities overall (i.e., lower \tilde{p}_{coh}) than their counterparts run in isolation (rows denoted A_1 and A_2 respectively). The discrepancy is not large, and could easily be explained by experimental differences, but alternatively may indicate that some cross-talk did indeed occur.